Computers and Chemical Engineering 156 (2021) 107554

Contents lists available at ScienceDirect

Computers and Chemical Engineering

journal homepage: www.elsevier.com/locate/compchemeng

Technical Note

Personalized medicine for GnRH antagonist protocol in *in vitro* fertilization procedure using modeling and optimal control

Apoorva Nisal[a,b], Urmila Diwekar[a,b,*], Elie Hobeika[c]

[a] Department of Industrial Engineering, University of Illinois, Chicago IL 60607, USA
[b] Center for Uncertain Systems: Tools for Optimization & Management (CUSTOM), Vishwamitra Research Institute, Crystal Lake IL 60012, USA
[c] Fertility Centers of Illinois, Chicago, IL, USA

ARTICLE INFO

Article history:
Received 26 April 2021
Accepted 27 September 2021
Available online 2 October 2021

Keywords:
Superovulation
IVF Treatment
Customized medicine
Crystallization
Optimal control
GnRH antagonist protocol

ABSTRACT

Infertility is an inability of those of reproductive age to become or remain pregnant within five years of exposure to pregnancy WHO. Since its inception in 1978, In vitro fertilization (IVF) has become the most resorted protocol for treating infertility. This article is focused on the first stage of IVF namely, superovulation. Superovulation is the drug-induced ovarian stimulation process to facilitate multiple ovulations per menstrual cycle. Thus, successful superovulation is the foundation for a successful IVF cycle. Despite the existence of general guidelines for dosage prescription, patient customized dosage protocols do not exist, and complications, such as overstimulation, do occur. To solve the limitations of the existing empirical system, a mathematical algorithm is developed to provide a customized model of superovulation owing to the size distribution of eggs (follicles/ oocytes) obtained per cycle as a function of the chemical interactions of the drugs used and the patient conditions during the cycle, to serve as a baseline for forecasting the outcome. A personalized medicine approach was previously presented based on mathematical modeling and optimal control for the agonist Long Lupron protocol of IVF(Nisal et al., 2020). This article is an extension of that work and describes the theory, modeling, and optimal control strategy to improve outcomes of IVF treatment for the antagonist Ganirelix (GnRH) protocol used in clinical practice. The validation of the procedure is performed using clinical data from the patients previously undergone IVF cycles. The data was available for 13 patients and customized patient-specific model parameters were obtained from the data. The model was used to predict follicle size distribution for all 13 patients for the remaining days of the cycle. It was found that the personalized models showed a strong fit with the clinically observed follicle size distribution (FSD). Then, the optimal control method was used for each individual patient to predict optimized drug dosage protocols using the customized patient specific parameters. The validity of modeling and optimization approach is corroborated by the results and show the efficacy of the optimized drug dosage protocols for each patient.

1. Introduction

Infertility is a disease affecting around 48 million couples and 186 million individuals globally (WHO, 2020). Around 2% women suffer from primary infertility and 10% women suffer from secondary infertility globally based on a survey conducted by the World Health Organization (WHO) using data from 190 countries over a 20 year time period. Primary infertility is the inability to conceive a first live birth and secondary infertility is the inability to conceive after a prior live birth. Developing regions and countries across the world and especially some regions of Eastern Europe, North Africa, the Middle East, Oceania, and Sub-Saharan Africa showed higher prevalence of infertility (Mascarenhas et al., 2012). In the United States, the Center for Disease Control (CDC) reported that 19% of women had primary infertility and 6.5% from secondary infertility while 12.7% of the women used infertility services based on data from the year 2015–2017 (CDC, 2019).

The in-vitro fertilization process is one of the most frequently adopted infertility treatments in Assisted Reproductive Technologies (ART) worldwide. More than 5 million babies have been born through in vitro fertilization techniques (Adamson et al., 2013) and in the United States 1.7% of the total infants were born through ART in 2015 (Sunderam et al., 2018). *In vitro* fertilization (IVF) is a process by which egg cells (oocytes) are fertilized by a sperm outside the body in a laboratory by simulating similar conditions in the body. Then, these fertilized eggs (embryos) are implanted back in the uterus for a full-term pregnancy. It has four basic stages

* Corresponding author.
E-mail address: urmila@vri-custom.org (U. Diwekar).

https://doi.org/10.1016/j.compchemeng.2021.107554
0098-1354/

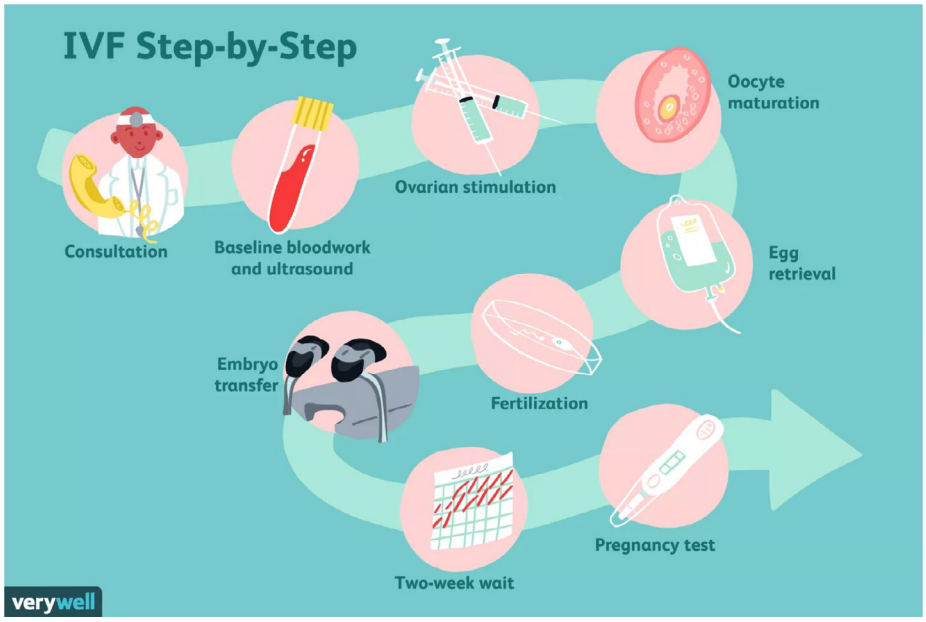

Fig. 1. Stages of *In vitro* Fertilization procedure (Roberts, 2020).

(Fritz and Speroff, 2010): superovulation, egg retrieval, insemination/fertilization and embryo transfer. An illustration of the process is shown in Fig. 1.

Regardless of the geographical location, IVF remains an expensive treatment to date with out-of-pocket estimates per cycle costing around $10,000-$15,000. This expense is variable and may increase with multiple factors such as unsuccessful IVF cycles, multiple births, low infant birth weight and preterm births owing to IVF cycles (Sunderam et al., 2018). The high costs of ivf are a result of the high cost of drugs, fixed costs for infrastructure and testing involved. Thus the cost of a successful IVF procedure hinges on the cost of superovulation. Currently, this step is executed using almost daily monitoring of the follicle development using ultrasound and blood tests. The daily dosage of hormones is customized for each patient based on these tests. Conventionally, doses are prescribed by clinicians based on empirical data instead of randomized trials and tend to start at 150 or 225 IU. Typically minimum dosages prescribed by clinicians start between 150–300 IU for younger patients and reach the absolute maximum at 450 IU for patients with poor response (Jungheim et al., 2015; Rombauts, 2007; Dorn, 2005). Devroey and team recorded a high number of retrieved oocytes even with an initial low dose FSH (Follicle Stimulating Hormone) (100 IU) on a relatively young age group (Devroey et al., 1998).

The decision making process behind choosing an FSH dose for a patient includes various markers such as age, anamnesis, clinical criteria and ovarian markers such as AFC (Antral Follicle Count) and AMH (Anti-Mullerian Hormone) (La Marca and Sunkara, 2013). Recent studies show that utilizing the marker AFC to determine the FSH starting dose showed that less than 225IU was required for most patients under the age of 35 years (La Marca et al., 2013). There are general guidelines for the dosage limits albeit, the optimization of dose for each patient is not attempted. IVF procedure with higher dosages can result in a condition such as the Ovarian Hyper Stimulation Syndrome (OHSS) (Alper et al., 2009), for which curative actions are still unidentified. Around 1–2% of women undergoing IVF suffer from a serious case of OHSS (Klemetti et al., 2005). The prevalence of Polycystic Ovarian Syndrome (PCOS) in patients has been shown to increase the incidence of OHSS and these patients are found to be the ones most susceptible to OHSS. Many patients without PCOS may also develop OHSS after stimulation. Protocols based on factors like age, AMH, AFC, FSH, BMI (Body Mass Index) levels and smoking history predict optimal protocols with the highest follicle yield and reduced occurrence of OHSS (Yovich et al., 2016).

Computational approaches have been developed recently to predict an IVF cycle's outcome depending on characteristics like patient characteristics, historical ivf cycle data, embryo morphology or biomarkers during culture to design a cost-effective customized treatment strategy. Post-treatment predictors included number of eggs collected, cryopreservation of embryos and embryonic stage when transferred (Simopoulou et al., 2018). Personalized treatment for IVF using the mathematical tool of æ̃nomogramg predicted the ovarian response and starting FSH dose based on predictors such as age, FSH, AMH and AFC (Allegra et al., 2017; Di Paola et al., 2018; La Marca et al., 2013; Moon et al., 2016; Papaleo et al., 2016). Variability in response based on indicators such as- FSH, LH/FSH ratio, AMH (Anti-Mullerian Hormone), BMI (Body Mass Index), AFC and age establish the complexity and diversity in biological and clinical features for each patient. The feature diversity in patients increases uncertainty towards the estimation of IVF outcomes, thus indicating the need for customized patient-specific and cycle-specific predictive models (Simopoulou et al., 2018).

All the existing protocols use patient history, monitoring and clinical judgement of the physician as the basis for dosage determination. The empirical nature of the process can increase the incidence of complications such as overstimulation or unsuccessful superovulation. The extensive infrastructure cost for testing and monitoring, along with the cost of medicines, multiply the expenses for superovulation stage.

These studies corroborate the need for a personalized IVF treatment and modules that can provide optimal patient-specific drug dosage profiles, which can reduce hyper-stimulation, cost of treatment, improve the oocyte quality and quantity, and thus increase the overall success rate of IVF, resulting in successful pregnancies and live-birth. This is the focus of our work.

There are four commonly used protocols for IVF. The four protocols (Scoccia, 2017) are (1) Long Lupron agonist Protocol, (2) Microflare agonist protocol, (3) Four stop Lupron agonist Protocol, and (4) Flexible GnRH antagonist (Ganerelix or Cetrorelix) Protocol.

Previously a mathematical modeling and computerized algorithmic approach to generate personalized hormonal dosing for augmented superovulation were presented for the Long Lupron agonist protocol (Nisal et al., 2020). In our recent work, we found that all agonist protocols behave in a manner similar to the Long Lupron Protocol as far as the modeling and optimization of the superovulation stage is concerned. However, antagonist protocol is different and is the focus of current endeavor. The work presented here builds on the foundation laid by the previous model. A customized model for the antagonist protocol using Ganirelix (GnRH) is presented here. Studies have shown that flexible GnRH administration generates higher quality mature follicles,significantly improve implantation, clinical pregnancy, and live birth rates in high responders and improve outcomes for patients with PCOS while reducing onsets of OHSS (Chern et al., 2020; Trenkić et al., 2016).

The validation of the procedure is carried out using clinical data from patients who have previously undergone IVF cycles. The follicle size data of the cycle along with the dosage is used to fit the patient parameters. These parameters are then used to calculate follicle distribution for each day using the customized model and compared with the actual data. This procedure was conducted for 13 patients. The results of the customized models are found to be closely matching with the observed FSD on the successive days of the IVF superovulation cycle. This customized model is then used to optimize the dosage for this patient. Using the model and the optimized dosage, the FSD at the end of the cycle was determined and compared with dosage specified by the doctors in these cycles.

The next section presents the modeling and optimal control methodology, followed by the results and discussions section. Section 4 presents the summary and future work.

2. Methodology

In the earlier work, principles of batch crystallization were used to develop a model for superovulation for the agonist protocol of IVF. The method of moments was used to represent the follicle growth and number prediction model (Yenkie et al., 2013; Nisal et al., 2020). This section presents the model briefly below, followed by the optimal control strategy.

2.1. mathematical modeling of in vitro fertilization

Superovulation is the first stage in IVF where the growth of multiple follicles is induced through administration of external hormonal injections resulting in follicle growth. The number of follicles activated for growth remains constant for any particular patient (Baird, 1987). There are marked similarities between the superovulation stage of IVF and the particulate process of batch crystallization(Hill, 2005; Yenkie and Diwekar, 2012). The moment model discussed here was developed on the basis that properties of a particulate system can be represented by moments of its particle size distribution, concepts of batch crystallization and resemblance of superovulation to growth of seeded batch crystals (Hill, 2005; Hu et al., 2005; Nisal et al., 2020; Randolph, 2012).

The moments are calculated using the baseline data for each patient and using the general expression in (1). Where μ_i is the ith moment, $n_j(r,t)$ is the number of follicles in bin 'j' of mean radius 'r' at time 't',r_j^i is the mean radius of jth bin and Δr_j is the range of follicle radii in each bin.

$$\mu_i = \sum n_j(r,t) r_j^i \Delta r_j \tag{1}$$

Before starting Ganirelix:

$$G(t) = k1\Delta C_{fsh(t)}^{\alpha 1} \tag{2}$$

After starting Ganirelix:

$$G(t) = k2\Delta C_{fsh(t)}^{\alpha 2} \tag{3}$$

$$\mu_0 = constant \tag{4}$$

$$\frac{d\mu_i}{dt} = iG(t)\mu_{i-1}(t);\ (i = 1, 2, \ldots 6) \tag{5}$$

The model for predicting follicle size and distribution utilizes follicle growth rate and moment equations. It is assumed that the follicle growth rate (G)) is directly dependent on the dose of FSH administered (ΔC_{fsh}) as shown in (2) and (3). Here, $k1$, $k2$ and $\alpha 1, \alpha 2$ are the rate constants and the rate exponents respectively. In case of the antagonist protocol, Ganirelix (GnRH) is administered on different cycle days depending on initial baseline date for each patient. Ganirelix is a gonadotropin releasing hormone antagonist (GnRH) used to delay premature ovulation and to help egg growth. To represent the antagonistic behavior of Ganirelix, the growth function was modified compared to previous study (Nisal et al., 2020).

Thus, the growth rate before Ganirelix is administered is as shown in (2) and the growth after Ganirelix is administered is as shown in expression (3).

For patients who were not administered Ganirelix, the protocol defaulted to the agonist protocol described in Nisal et al. (2020) thus only using the growth function as shown in (2). The moment equations for calculating moments from the zeroth moment up to the 6^{th} order were derived from the general expressions in (4) and (5). It can be seen from (5) that the $(n+1)$th moment is dependent on the nth moment.

In in vitro fertilization process, the measurements for follicle size and growth are conducted on different cycle days to observe sufficient growth. In clinical settings, the follicles are grouped by size in 6 bins ranging from 0-24mm in diameter during a single measurement. Thus, six moment values can be obtained per day. The values of patient specific parameters $k_1, k_2, \alpha_1, \alpha_2$ were obtained by mean squared minimization of calculated moments versus the observed moments extracted from experimental FSD. The moment values predicted by Eqs. (4) and (5) are converted to follicle size distribution (FSD) to validate the output. The follicle distribution was approximated by using an inversion matrix (A) combined with non-linear optimization techniques as shown in Eq. (6) and (7) (Flood, 2002; Yenkie et al., 2013).

$$\mu = An \tag{6}$$

$$n = A^{-1}\mu \tag{7}$$

Where, n - vector of the number of follicles in all size bins for the ith cycle day, μ - moment vector for ith cycle day and **A** - inversion matrix of size 6x6. The inversion matrix is shown in Table 2 (Appendix).

In the clinical (experimental) settings, the initial dosage for the patient is determined by the physician based on various patient factors. For the first four days of the cycle, same dose is continued. After the 4^{th} day, blood testing and ultrasound tests are used to determine dose for each day. The validity of the model was evaluated by comparing the follicle size distribution as predicted by the model from 5^{th} day on with that of the experimental data.

2.2. Optimal control

The optimal control approach evaluates the time-varying values of control variables which aid in achieving the desired outcome. The optimized variable in an optimal control problem is a time varying vector which makes the optimal control approach appropriate for predicting customized dosages over time. Optimal control can be applied to problems in the biomedical field include- predicting cancer chemotherapy and tumor degradation

(Castiglione and Piccoli, 2007; Czakó et al., 2017), drug scheduling in HIV infection treatment (Khalili and Armaou, 2008) and blood glucose regulation in insulin-dependent diabetes patients (Acikgoz and Diwekar, 2010). The maximum principle method for optimal control is applied here which is one of the different methods for solving optimal control problems like- calculus of variations, dynamic programming, maximum principle, and nonlinear programming (Diwekar, 2008). The maximum principle method solution is obtained through solving first order ordinary differential equations thus making the process easier as compared to other methods. The control variable is the value of hormonal doses per day of the IVF cycle. The objective of superovulation is to obtain a high number (maximum possible) of uniformly sized (18–22 mm diameter) follicles on the last day of FSH administration.

2.2.1. Mathematical formulation

After initial 4–5 days of treatment with FSH, the follicle size and number plots follow Gaussian/ Normal distribution and this trend continues with a shift in mean and variance. Also, the patient data shows the normal distribution; thus, it was assumed as an apriori distribution for follicles. The normal distribution is used to define the objective function in terms of moments. The moment model for FSD prediction, as discussed above, and the method for deriving normal distribution parameters are used as the basis for deriving expressions for the mean and coefficient of variation. The coefficient of variation and mean of the normal distribution expressed in terms of moments are derived using the method presented by John et al. (2007). The mean ($\bar{x}$) and coefficient of variation (CV) for the normal distribution of follicle size expressed in terms of moments are shown in Eq (8) and (9).

$$\bar{x} = \frac{\mu_1}{\mu_0} \tag{8}$$

$$CV = \sqrt{\frac{\mu_2 \mu_0}{\mu_1^2} - 1} \tag{9}$$

The objective of superovulation is to generate uniformly sized follicles on the last day of the cycle. Thus, the objective of superovulation in mathematical form can be; to minimize the coefficient of variation on last day of FSH administration ($CV(t_f)$) where the control variable is the dosage of FSH with time ($C_{fsh}(t)$). To customize the model for each patient, the parameters are evaluated using the initial two-day observations of the follicle size and counts along with the FSH administered. The optimal dosage prediction for the desired superovulation outcome is represented as Eq. (10). The objective function is subject to the follicle growth term and moment model constraint, equation for the coefficient of variation in terms of moments and mean as presented in Eqs. (11) and (12) and the constraint on mean follicle size ($\bar{x}$) to not exceed beyond 22mm diameter.

$$\min C_{fsh} CV(t_f) \tag{10}$$

s.t.

$$\frac{dCV}{dt} = \frac{G\mu_0}{CV\mu_1}\left[1 - \frac{\mu_2 \mu_0}{\mu_1^2}\right] \tag{11}$$

$$\frac{d\bar{x}}{dt} = G \tag{12}$$

2.2.2. Maximum principle method

The optimal control problem presented here has nine state variables with nine state equations. In the maximum principle method of optimal control, one adjoint variable corresponding to one state variable is introduced resulting in nine adjoint variables with nine adjoint equations. The ith state variable is denoted as $'y_i'$ and the nine state variables are shown in Eq. (13). The ith adjoint variable is denoted as $'z_i'$. Then the objective is converted to the Hamiltonian form(H), which on expansion involves both state and adjoint variables. These expressions are shown in Eq. (14) to (17). The optimality condition for this problem and tolerance level for the derivative of Hamiltonian with respect to control variable is expressed in Eq. (18). The expressions presented in this section are similar to those presented previously (Nisal et al., 2020) with the exception of the growth function as described in the previous subsection. Appropriate growth function is used depending on the start time of Ganrirelix(GnRH).

$$y_i = [\mu_0, \mu_1, \mu_2, \mu_3, \mu_4, \mu_5, \mu_6, CV, \bar{x}] \tag{13}$$

$$Max_{C_{fsh(t)}}[-y_8(t_f)] \tag{14}$$

$$\frac{dy_i}{dt} = f(y_i, t, C_{fsh}) \tag{15}$$

$$\frac{dz_i}{dt} = \sum_{j=1}^{9} z_i \frac{\delta f(y_i, t, C_{fsh})}{\delta y_i} = f(y_i, t, C_{fsh}) \tag{16}$$

$$H = \sum_{j=1}^{9} z_i f(y_i, t, C_{fsh}) \tag{17}$$

$$\left|\frac{dH}{dC_{fsh}}\right| = 0 \tag{18}$$

This set of equations are solved stepwise. The state equations are integrated in forward direction from starting time t_0 till the end of the cycle t_f and the adjoint equations are integrated backward. At each time step it is verified that the optimality condition is satisfied.

2.3. Estrogen modeling

As the oocytes or follicle growth occurs, estrogen is released. Thus, increased levels of estrogen, indicate that follicle growth is occurring and is used as a metric by clinicians to observe healthy growth. Thus, the growth of follicles and follicles release estrogen while growing. Since the estrogen growth depends on maturity of follicles and is changing with the follicle size distribution, we found that the moment which is related to volume of the follicle (i.e. third moment, μ_3), can be correlated to estrogen. This is represented mathematically in the model by the expression in (19). Where, F(t) represents the growth of estrogen and the volume of follicles is represented by the third moment (μ_3).

$$F(t) = \beta_1 * \mu_3 \pm \beta_2 \tag{19}$$

3. Results & discussion

The models presented above were applied to the 13 patients from the University of Illinois at Chicago IVF center. The data included details like prescribed dose profile, follicle measurements on different cycle days, patient age, previous infertility, or pregnancy for different women. The initial prescribed dose, follicle measurements, cycle time and, Ganirelix start day were the only inputs to the model. An example of utilized input data for a Patient is presented in Table 1.

The mathematical model results fit against available clinical data, parameter estimation, estrogen modeling, and optimal control are presented and discussed in this section.

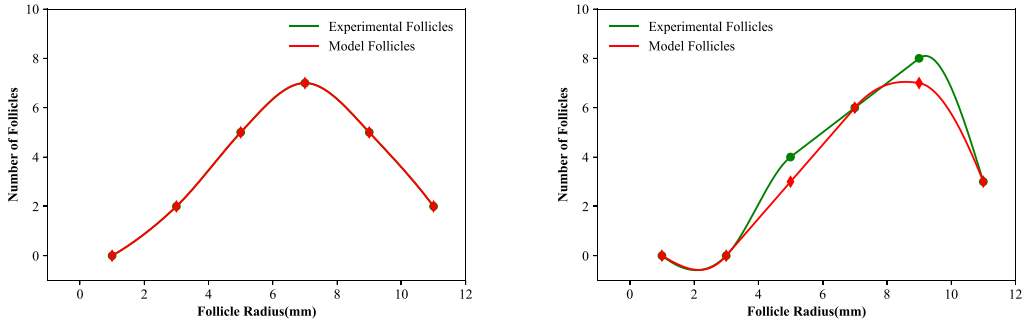

Fig. 2. Comparison of Observed (Experimental Follicles) Follicular Distribution with the Follicle Size Distribution Predicted by Customized Model (Model Follicles) for Various Days for Patient 8 (a) Day 10 and (b) Day 11.

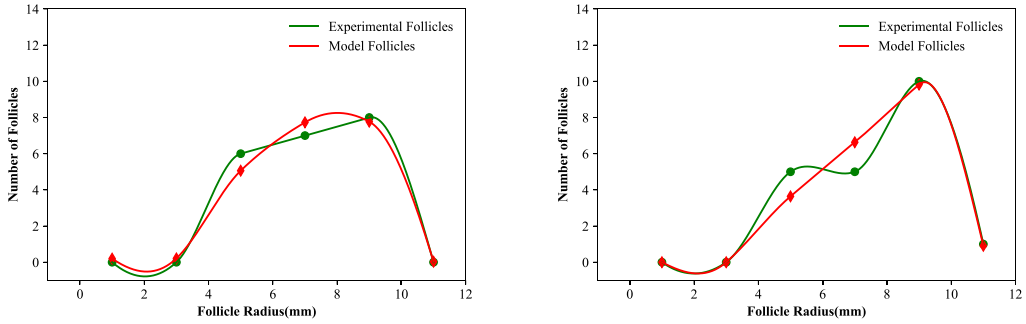

Fig. 3. Comparison of Observed (Experimental Follicles) Follicular Distribution with the Follicle Size Distribution Predicted by Customized Model (Model Follicles) for Various Days for Patient 12 (a) Day 11 and (b)Day 12.

Table 1
Tabular representation of Number of Follicles observed and the prescribed dosages on different cycle days for a patient.

Number of Follicles						
Day bins/day	1	5	7	8	9	11
0-4	6	2	0	0	0	0
4-8	3	2	0	0	0	0
8-12	3	8	6	6	5	2
12-16	0	0	5	5	5	5
16-20	0	0	1	1	2	3
20-24	0	0	0	0	0	2
GnRH Day	6					
$C_{fsh}(IU)$	337.5	187.5	112.5	112.5	112.5	37.5

3.0.1. Model validation

The mathematical model described in previous section uses the data collected on all cycle days to calibrate the model. It is crucial to examine the performance of the model on various cycle days and observe the fit against experimental data. The follicle size distribution (FSD) for two consecutive cycle days observed in real practice (marked as experimental) and compared to the model predictions (marked as model) for patient 8 and 12 are shown in Figs. 2 and 3. Fig. 2.a and b show the comparison of FSD observed in experimental data to the model predictions for patient 8 on cycle day 10 and 11 respectively. Similarly, Fig. 3.a and b show the comparison of FSD observed in experimental data to the model predictions for patient 12 on cycle day 11 and 12 respectively. It is observed from these results that the model performs very well for these patients.

The results of these two patients are selected as they represent two different start times for Ganirelix. In case of patient 8, Ganirelix was started on day 6 of the cycle, where as for patient 12, the Ganirelix was administered on day 8 of the cycle.

A histogram of the ratio of total mature follicles on the last cycle day predicted by the model (indicated as M) to the total mature

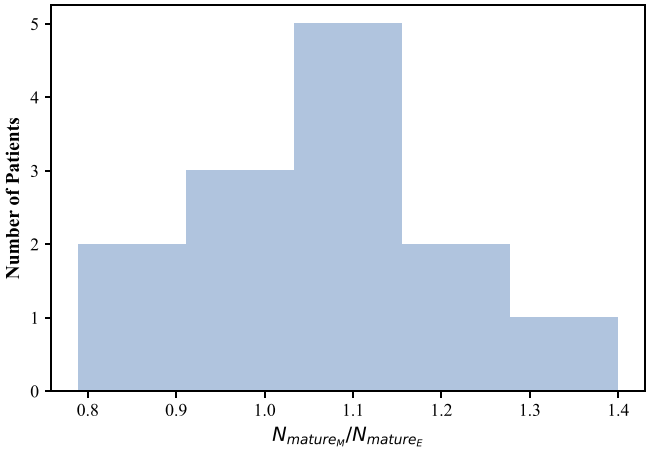

Fig. 4. Histogram of $(n_{mature,\ M})/(n_{mature,\ E})$ for 13 patients on the last day of the cycle.

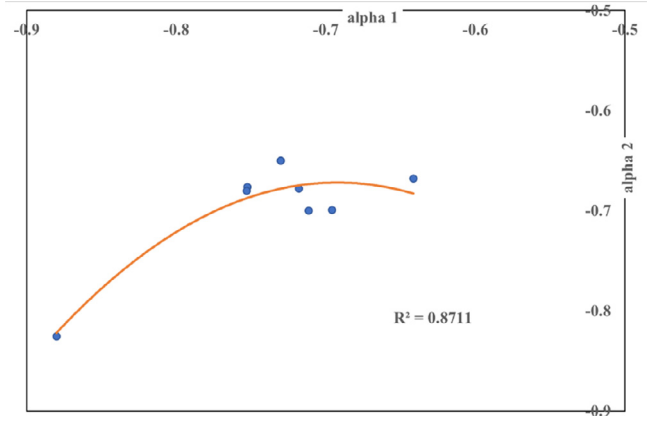

Fig. 5. Fit for the Patient Parameter $\alpha 1$ versus $\alpha 2$.

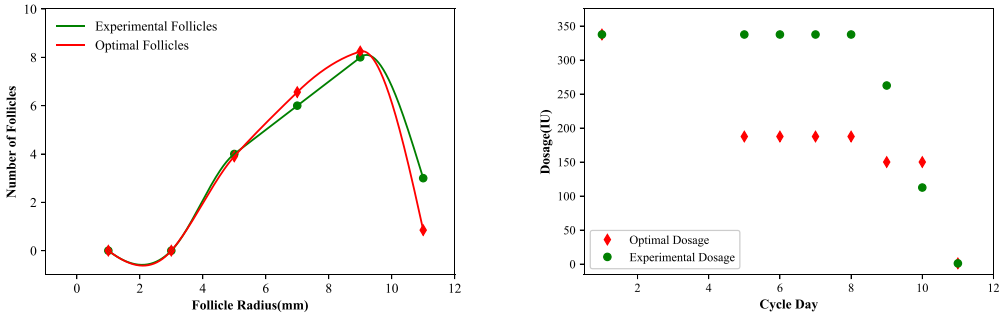

Fig. 6. (a) Follicular distribution for Patient 8 predicted by optimal control vs observed follicle distribution from experiments for the last day of the cycle (b) Optimal dosage for Patient 8 predicted by optimal control vs experimental dosage prescribed by the clinician.

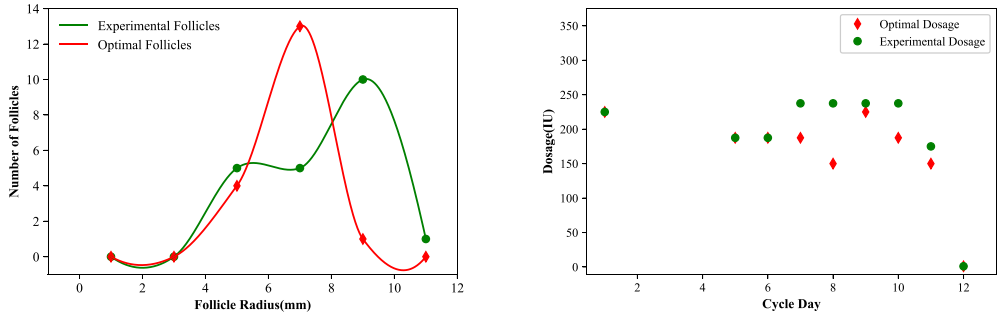

Fig. 7. (a) Follicular distribution for Patient 12 predicted by optimal control vs observed follicle distribution from experiments for the last day of the cycle (b) Optimal dosage for Patient 12 predicted by optimal control vs experimental dosage prescribed by the clinician.

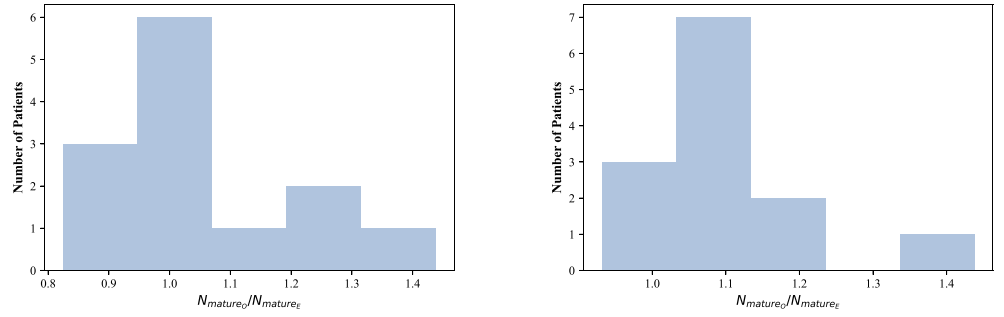

Fig. 8. Histogram of $(n_{mature,\ O})/(n_{mature,\ E})$ for 13 patients (a) On the last day of the cycle (b) Shifted histogram for next day after last cycle day.

follicles observed on the last cycle day experimentally (indicated as E) was created to evaluate the prediction accuracy of the model. As seen in Fig. 4, the model predicted follicular outcomes same as observed experimentally for 77% of the patients. The model predicted better follicular outcomes compared to experimental data for 15% of the patients and marginally worse than experimental data for 7% of the patients. As stated earlier, data were acquired for 13 patients from Fertility Center of Illinois, Chicago, IL USA. This data is used to study the predictive capability of the model for the final day of stimulation.

3.1. Results from parameter estimation

It has been observed previously that the model parameter k (follicle growth rate constant) is uniform across all patients (Nisal et al., 2020). Similar trends were also observed in this study. The growth rate constant before Ganirelix ($k1$) and the growth rate constant after Ganirelix ($k2$) were observed to be constant and independent of the patient. Thus, the follicle growth rate constants with the Ganirelix protocol have been observed to be patient independent.

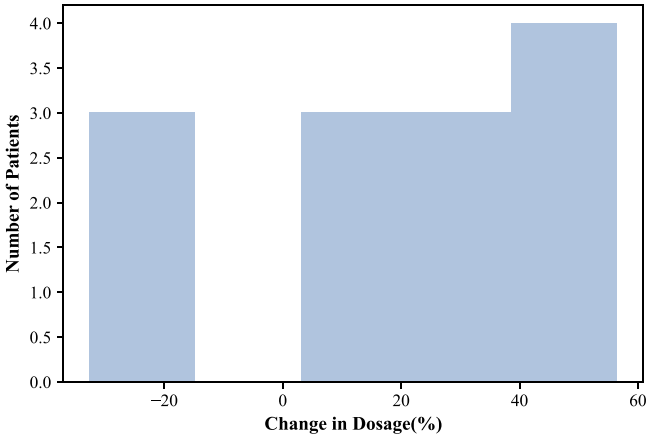

Fig. 9. Histogram of % Reduction in Dosage for 13 patients.

Although $\alpha 1, \alpha 2$ (follicle growth rate exponents) change for each patient, it is observed that $\alpha 2$ has a non-linear relationship with $\alpha 1$ of the polynomial of the order two as shown in Fig. 5.

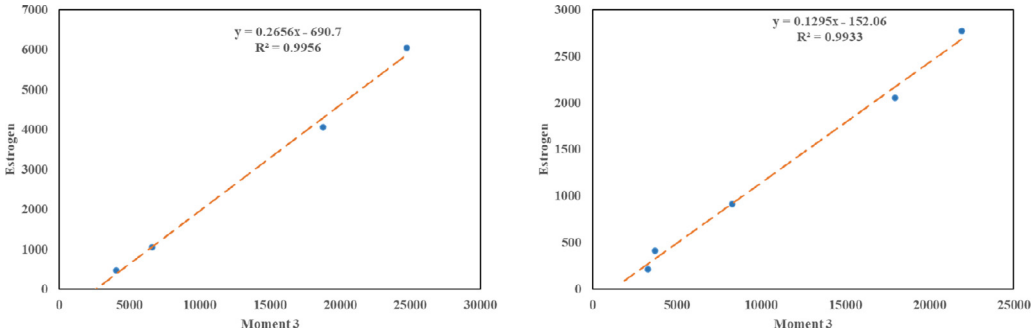

Fig. 10. Comparison of Estrogen Observed Experimentally to the 3^{rd} moment for (a) Patient 8 (b) Patient 12.

Only one patient data was observed to be an outlier with values of $\alpha 1$ and $\alpha 2$ as -0.77 and -0.85, respectively. This data was removed from further analysis and the accuracy of the resulting fit was found to be 87.11% as shown in Fig. 5. It can be concluded that the model is the best fit for values of both the rate exponents, alpha1 and alpha2 ranging from -0.85 to -0.6. It should be noted that the model presented here is identifiable for values of alpha between (-1, 0).

This current study utilizes data available for all cycle days to make predictions. However, to realize this model in the clinical settings, it is important to utilize initial 2-day data by only taking measurements on 1st and 5th cycle day to minimize testing and diagnostic costs. Since,the growth rate constants before and after Ganirelix ($k1, k2$) have constant values and there exists a non-linear relationship between $\alpha 1$ and $\alpha 2$; values for $\alpha 2$ can be obtained when rest of the 3 parameters are known. Thus, the existence of a relationship between $\alpha 1$ and $\alpha 2$ is important to consider the initial 2-day data for patient-specific parameter predictions and then to use this data to find the optimal dosage profile.

3.2. Optimal control

The dosage for patients changes throughout the cycle depending on the start time of Ganirelix as described previously in Section 2. The maximum principle method for Optimal control is applied to find dosage from 5th day onward. The patient parameters estimated using the all-day data are used and the maximum principle method is applied to determine dosage from the start day for Ganirelix. The optimal drug dosages for each patient are calculated based on the starting dose, cycle days, Ganirelix start day and the initial follicle size distribution observed in each patient. Finally, the total mature follicles on the final day using optimal control are then compared to the observed mature follicles using the dosage specified. The model is personalized for each patient by considering all-day data consisting of follicle measurements and prescribed doses from that patient. After that, the optimal control approach was applied to calculate the optimal dosage profile for that patient.

The optimal control results for patients 8 and 12 are shown in Figs. 6 and 7 respectively. Figs. 6.a and 7.a show the mature follicle distribution optimal versus experimental follicle distribution for patients 8 and 12 respectively. While Figs. 6.b and 7.b show the optimal dosage versus experimental dosage for patients 8 and 12. The cumulative dose for patient 8 is found to be 2401 IU compared to the clinician prescribed dose of 3076 IU. The cumulative dosage for patient 12 was found to be 2101 IU as opposed to the prescribed dosage of 2326 IU. The total number of mature follicles for patient 12 was slightly lower with optimal dosage (total 15 follicles) compared to mature follicles with experimental dosage (16 follicles). However, the model prediction shows that waiting for 1 day to harvest the follicles will increase the total follicle count to 18 follicles even with the lower dosage. Thus, asserting the validity of these results.

These results exemplify the notable reduction in dosage from the customized model and consequent reduction in the costs to the patient. The initial data for 13 patients, along with the results from optimal control for all the patients, is presented in Table 3 attached in the appendix. 1 patient was excluded from the analysis due to insufficient initial data. The table shows the age of each patient, values for parameters- K1, K2, $\alpha 1$, and $\alpha 2$, experimentally observed follicles, model predicted optimal follicles on the last cycle day, cumulative dosage prescribed by the clinician, and dosage predicted by the model.

The optimal control profile was calculated and customized for each patient for the clinical data available on 13 patient cycles. A histogram of the ratio of final day mature follicles predicted by the model with optimal dosage ($n_{mature,\ O}$) to final day mature follicles observed experimentally ($n_{mature,\ E}$) in real practice is presented in Fig. 8. As shown in Fig. 8.a, for 85% of the total patients, the model predicts better follicle outcomes with optimal dosage compared to experimental data. Although, the model predictions are not as good for the rest of the 15% of the patients, Fig. 8.b shows that waiting for one day to harvest the follicles, results in all of the patients showing better mature follicle outcomes using optimal dosage compared to as observed experimentally.

The histograms of percentage (%) reduction in dosage for each patient are presented in Fig. 9. 77% of these patients also show a significant reduction (20%-60%) in the cumulative dose requirements for successful superovulation while the remaining 23% require a marginally higher optimal dosage ($>= 20\%$) than the physician prescribed dosage.

Excessive dosages of fertility medications such as FSH or Ganirelix increase the risk of a potentially life threatening condition called the Ovarian Hyperstimulation Syndrome (OHSS) in patients. Thus, the incidence of OHSS is highly correlated with the higher dosages of FSH and Ganirelix. Although, OHSS is not considered as a parameter in the objective function for this study, the optimal dosages forecasted by the model are considerably lower than the prescribed dosages. Hence it can be concluded that the lower optimal doses comply with minimizing the onset of OHSS. The results presented in this section are tabulated in Table 3 (Appendix). Table 3 shows the patient id, $\alpha 1$, $\alpha 2$, experimentally observed mature follicles, total mature follicles predicted by the model, optimal follicles predicted by model and prescribed dosage, optimal dosage.

3.3. Estrogen modeling

The levels of the estrogen hormone show high correlation with the follicular volume or 3^{rd} moment (μ_3). Thus, the growth of the follicles should also show the growth of estrogen in patients as described in Section 2. Fig. 10.a and b shows the estrogen observed experimentally compared to the 3^{rd} moment for patient 8 and pa-

tient 12. It is observed that the estrogen modeling is patient dependent and the values for the constants $\beta 1$ and $\beta 2$ change for each patient. The high accuracy (R^2) values of 99% for both patients show that estrogen is highly correlated with follicle volume. Thus, it can be concluded that the model can predict estrogen levels in all the patients.

The observed estrogen on each cycle day for every patient along with the calculated third moment is presented in Table 4. The resulting patient specific relationship between Estrogen count and Third Moment along with respective (R^2) values for each patient is also presented in Table 5. These results also show that the estrogen can be used as a metric by clinicians to verify the success and regular progression of the ivf process.

4. Summary and future work

In vitro fertilization (IVF) has become a ubiquitous and recurrent method in assisted reproductive technology. The first stage (Superovulation) in ivf consists of drug-induced interventions to enable multiple ovulation in a menstrual cycle.Thus, the success of the entire IVF cycle hinges on the success of superovulation which is defined by the number and uniformly high quality of eggs retrieved in a cycle. The high cost of the IVF process is associated with the high cost of drugs and testing required during this stage. The progression of follicular development is observed daily using ultrasound and blood tests. In clinical practice, these tests determine the daily dosage of hormones for each patient. Although there are general guidelines for the dosage, the dose is not optimized for each patient. The cost of testing and drugs make this stage very expensive. A predictive model based approach was presented for customized medicine for an antagonist protocol using Ganirelix for IVF to control the monetary and physiological expense limitation of the system. The control strategy uses customized models for each patient based on all-day data from each patient to define the outcomes. An optimal control approach is then used on these customized models to obtain drug dosage profiles for each patient. The findings show that the procedure provides better odds for patients in terms of a higher number of mature follicles and reduced dosage. Thus, subsequently reducing the testing and associated costs. The process can also reduce the side effects of the drugs significantly. All day data was used in this study to predict optimal dosage protocols and observe follicle outcomes using those doses. However, it is imperative to minimize testing and diagnostic procedures to further reduce testing costs and thus necessitating an approach utilizing only 2-day data. In the current study, patient specific parameters $k1, k2$ are constant, and $\alpha 2$ is dependent on $\alpha 1$. Thus, 2-day data can be utilized with the current model. Although, the results for only 13 patients are presented in this study, a small clinical trial with 26 patients was subsequently conducted and the results are consistent with those presented here. This will be evaluated in the further and this approach will be extended to more patient data in the United States.

Declaration of Competing Interest

None.

Acknowledgements

We thank the Institutional Review Board at UIC for approving the current research to meet the requirements of Protection of Human Subjects research under Protocol #2012-0317 titled 'Understanding the Superovulation Stage of IVF Process for Optimal Drug Delivery'.

Appendix A

Tables 2-5

Table 2
Inversion Matrix **A**.

A					
2	6	10	14	18	22
2	18	50	98	162	242
2	54	250	686	1458	2662
2	162	1250	4802	13122	29282
2	486	6250	33614	118098	322102
2	1458	31250	235298	1062882	3543122

Table 3
Table presenting initial available data and results from mathematical model and optimal control model. Initial Data: ID - Patient ID, Exp Fol - Experimentally Observed Follicles Results from Parameter Estimation: $\alpha 1$- values for parameter $\alpha 1$ for each patient $\alpha 2$- values for parameter $\alpha 2$ for each patient Results from Mathematical Model: Model Fol - Follicles predicted by the mathematical model to evaluate model fit Results from Optimal Control: Opt Fol - Optimal Follicles predicted by model Presc. Dose (IU) - Dosage prescribed by clinician Opt Dose (IU)- Optimal Dosage predicted by model.

Patient ID	$\alpha 1$	$\alpha 2$	Exp fol	Model Fol	Opt fol	Exp Dose (IU)	Opt Dose(IU)
1	-0.66		10	10	12.01	4800	2512.5
2	-0.73	-0.65	13	14	12.42	3113.5	2476
3	-0.69	-0.69	11	13	12	3263.5	2213.5
5	-0.77	-0.85	16	17	23	946.75	1163.5
7	-0.75	-0.67	10	14	12	2252	2138.5
8	-0.71	-0.67	17	16	15.65	3076	2401
9	-0.64	-0.66	11	10	10.69	5850	3413.5
10	-0.71	-0.7	48	50	50	1188.5	1576
11	-0.75	-0.68	10	11	8.25	3301	2513.5
12	-0.88	-0.83	16	17	14	2326	2101
13	-0.65		19	15	18.04	5100	2437.5
14	-0.73		14	13	13.33	6375	2775
15	-0.68		23	28	24.08	2437.5	3112.5

Table 4
Table presenting available patient data for Estrogen and result from mathematical model-Third moment. Initial Data: ID - Patient ID, Cycle day, Estrogen. Results from Mathematical Model: Calculated Third Moment.

Patient ID	Cycle Day	Estrogen (E)	Third Moment (M)
1	1		924
1	5	724	3402.4
1	7	1941	5874.2
1	8	2089	6854.85
1	9	2766	7946.82
1	11	4695	12292.2
2	1		1232
2	5	467	2201.36
2	7	746	4890.57
2	10	2922	14670.03
2	11	4398	18303.05
3	1		1618
3	5	695	3832.51
3	7	874	6732.82
3	10		15075.65
3	11	1343	18754.28
5	1		1310
5	5	1975	5994.48
5	7	4459	17866.12
5	8	6868	19590.05
5	9	5084	21422.33
7	1	31.7	1124
7	5	404	2774.65
7	7	474	4503.01
7	10	1779	14125.63
7	11	2759	18142.07
8	1		902
8	5	466	3866.23
8	7	1054	8258.16
8	10	4061	21210.19
8	11	6056	25972.57
9	1	24	1174
9	5	285	4136.29
9	8		7196.06
9	11		11611.09
9	12	2531	13562.81
10	1		2996
10	5	1940	12256.98
10	7	3599	24648.73
10	10	11193	53364.25
11	1	64.5	1068
11	7	294	2386.68
11	10	997	7403.24
11	12	2153	16527.16
12	1		1894
12	5	217	3084.98
12	7	416	3861.59
12	9	914	7381.83
12	11	2058	17205.63
12	12	2778	24199.84
13	1		840
13	7	582	2829.11
13	9	1527	9333.64
13	12	4955	29208.05
14	1	47	982
14	5	191	3149.83
14	7	438	5092.19
14	9	741	7791.26
14	10	1419	9563.35
14	12	2686	17253.17
15	1	24	264
15	5	337	3555.25
15	7	1251	9680.75
15	10	4792	26322.79

Table 5
Table presenting results from Estrogen Modeling Initial Data: ID - Patient ID Results from Estrogen Modeling: Relationship between Estrogen(E) and Third Moment (denoted as M in Equation), R^2 value of fit.

Patient ID	Relationship between Estrogen(E) and Third Moment(M)	R
1	E = 0.3499*M - 76.844	0.9905
2	E = 0.2496*M - 198.74	0.9562
3	E = 0.0452*M + 543.42	0.9938
5	E = 0.2728*M + 1027.9	0.7716
7	E = 0.1284*M - 78.369	0.9314
8	E = 0.2656*M - 690.7	0.9956
9	E = 0.2034*M - 316.19	0.993
10	E = 0.1917*M + 958.41	0.9995
11	E = 0.15*M - 119.41	0.9775
12	E = 0.1295*M - 152.06	0.9933
13	E = 0.2736*M - 425.23	0.9996
14	E = 0.1661*M - 271.2	0.968
15	E = 0.2219*M - 255.11	0.9934

Supplementary material

Supplementary material associated with this article can be found, in the online version, at doi:10.1016/j.compchemeng.2021.107554.

References

Acikgoz, S.U., Diwekar, U.M., 2010. Blood glucose regulation with stochastic optimal control for insulin-dependent diabetic patients. Chem. Eng. Sci. 65 (3), 1227–1236. doi:10.1016/j.ces.2009.09.077.

Adamson, G.D., Tabangin, M., Macaluso, M., de Mouzon, J., 2013. The number of babies born globally after treatment with the assisted reproductive technologies (art). Fertil. Steril. 100 (3), S42.

Allegra, A., Marino, A., Volpes, A., Coffaro, F., Scaglione, P., Gullo, S., La Marca, A., 2017. A randomized controlled trial investigating the use of a predictive nomogram for the selection of the FSH starting dose in IVF/ICSI cycles. Reprod. Biomed. Online 34 (4), 429–438. doi:10.1016/j.rbmo.2017.01.012.

Alper, M.M., Smith, L.P., Sills, E.S., 2009. J. Exp. Clin. Assist.Reproduct. 6.

Baird, D.T., 1987. A model for follicular selection and ovulation: lessons from superovulation. J. Steroid Biochem. 27 (1–3), 15–23.

Castiglione, F., Piccoli, B., 2007. Cancer immunotherapy, mathematical modeling and optimal control. J. Theor. Biol. 247 (4), 723–732. doi:10.1016/j.jtbi.2007.04.003.

CDC, 2019. NSFG - Listing I - Key Statistics from the National Survey of Family Growth. Centers for Disease Control and Prevention.

Chern, C.-U., Li, J.-Y., Tsui, K.-H., Wang, P.-H., Wen, Z.-H., Lin, L.-T., 2020. Dual-trigger improves the outcomes of in vitro fertilization cycles in older patients with diminished ovarian reserve: aretrospective cohort study. PLoS ONE 15 (7), e0235707.

Czakó, B., Sápi, J., Kovács, L., 2017. Model-based optimal control method for cancer treatment using model predictive control and robust fixed point method. In: 2017 IEEE 21st International Conference on Intelligent Engineering Systems (INES). IEEE, pp. 000271–000276. doi:10.1109/INES.2017.8118569.

Devroey, P., Tournaye, H., Van Steirteghem, A., Hendrix, P., Out, H.J., 1998. The use of a 100 IU starting dose of recombinant follicle stimulating hormone (puregon) in in-vitro fertilization. Hum. Reprod. 13 (3), 565–566. doi:10.1093/humrep/13.3.565.

Di Paola, R., Garzon, S., Giuliani, S., Laganà, A.S., Noventa, M., Parissone, F., Zorzi, C., Raffaelli, R., Ghezzi, F., Franchi, M., et al., 2018. Are we choosing the correct FSH starting dose during controlled ovarian stimulation for intrauterine insemination cycles? potential application of a nomogram based on woman's age and markers of ovarian reserve. Arch. Gynecol. Obstet. 298 (5), 1029–1035. doi:10.1007/s00404-018-4906-2.

Diwekar, U., 2008. Introduction to Applied Optimization, 22. Springer Science & Business Media.

Dorn, C., 2005. Fsh: what is the highest dose for ovarian stimulation that makes sense on an evidence-based level? Reprod. Biomed. Online 11 (5), 555–561. doi:10.1016/S1472-6483(10)61163-7.

Flood, A., 2002. Thoughts on recovering particle size distributions from the moment form of the population balance. Dev. Chem. Eng. Miner.Process. 10 (5–6), 501–519. doi:10.1002/apj.5500100605.

Fritz, M.A., Speroff, L., 2010. Clinical Gynecologic Endocrinology and Infertility. Lippincott Williams & wilkins.

Hill, P., 2005. Batch crystallization. In: Korovessi, E., Linninger, A.A. (Eds.), Batch Processes. Taylor and Francis, CRC Press, New York, USA, pp. 163–216.

Hu, Q., Rohani, S., Jutan, A., 2005. Modelling and optimization of seeded batch crystallizers. Comput. Chem. Eng. 29 (4), 911–918. doi:10.1016/j.compchemeng.2004.09.011.

John, V., Angelov, I., Öncül, A., Thévenin, D., 2007. Techniques for the reconstruction of a distribution from a finite number of its moments. Chem. Eng. Sci. 62 (11), 2890–2904. doi:10.1016/j.ces.2007.02.041.

Jungheim, E.S., Meyer, M.F., Broughton, D.E., 2015. Best practices for controlled ovarian stimulation in in vitro fertilization. In: Seminars in Reproductive Medicine, 33. Thieme Medical Publishers, pp. 077–082. doi:10.1055/s-0035-1546424.

Khalili, S., Armaou, A., 2008. Sensitivity analysis of HIV infection response to treatment via stochastic modeling. Chem. Eng. Sci. 63 (5), 1330–1341. doi:10.1016/j.ces.2007.07.072.

Klemetti, R., Sevón, T., Gissler, M., Hemminki, E., 2005. Complications of IVF and ovulation induction. Hum. Reproduct. 20 (12), 3293–3300. doi:10.1093/humrep/dei253.

La Marca, A., Grisendi, V., Giulini, S., Argento, C., Tirelli, A., Dondi, G., Papaleo, E., Volpe, A., 2013. Individualization of the FSH starting dose in IVF/ICSI cycles using the antral follicle count. J. Ovarian Res. 6 (1), 11. doi:10.1186/1757-2215-6-11.

La Marca, A., Sunkara, S.K., 2013. Individualization of controlled ovarian stimulation in IVF using ovarian reserve markers: from theory to practice. Hum. Reprod. Update 20 (1), 124–140. doi:10.1093/humupd/dmt037.

Mascarenhas, M.N., Flaxman, S.R., Boerma, T., Vanderpoel, S., Stevens, G.A., 2012. National, regional, and global trends in infertility prevalence since 1990: a systematic analysis of 277 health surveys. PLoS Med. 9 (12), 1–12. doi:10.1371/journal.pmed.1001356.

Moon, K.Y., Kim, H., Lee, J.Y., Lee, J.R., Jee, B.C., Suh, C.S., Kim, K.C., Lee, W.D., Lim, J.H., Kim, S.H., 2016. Nomogram to predict the number of oocytes retrieved in controlled ovarian stimulation. Clin. Exp. Reprod. Med. 43 (2), 112–118. doi:10.5653/cerm.2016.43.2.112.

Nisal, A., Diwekar, U., Bhalerao, V., 2020. Personalized medicine for in vitro fertilization procedure using modeling and optimal control. J. Theor. Biol. 487, 110105.

Papaleo, E., Zaffagnini, S., Munaretto, M., Vanni, V.S., Rebonato, G., Grisendi, V., Di Paola, R., La Marca, A., 2016. Clinical application of a nomogram based on age, serum FSH and AMH to select the FSH starting dose in IVF/ICSI cycles: a retrospective two-centres study. Eur. J. Obstetr. Gynecol.Reproduct. Biol. 207, 94–99. doi:10.1016/j.ejogrb.2016.10.021.

Randolph, A., 2012. Theory of Particulate Processes: Analysis and Techniques of Continuous Crystallization. Elsevier.

Roberts, E., 2020. IVF Step by Step.

Rombauts, L., 2007. Is there a recommended maximum starting dose of FSH in IVF? J. Assist. Reprod. Genet. 24 (8), 343–349. doi:10.1007/s10815-007-9134-9.

Scoccia, H., 2017. IVF Program Protocols for Assisted Reproductive Technologies. University of Illinois at Chicago.

Simopoulou, M., Sfakianoudis, K., Antoniou, N., Maziotis, E., Rapani, A., Bakas, P., Anifandis, G., Kalampokas, T., Bolaris, S., Pantou, A., et al., 2018. Making IVF more effective through the evolution of prediction models: is prognosis the missing piece of the puzzle? Syst. Biol. Reprod. Med. 64 (5), 305–323. doi:10.1080/19396368.2018.1504347.

Sunderam, S., Kissin, D.M., Crawford, S.B., Folger, S.G., Boulet, S.L., Warner, L., Barfield, W.D., 2018. Assisted reproductive technology surveillanceunited states, 2015. MMWR Surveill. Summ. 67 (3), 1. doi:10.15585/mmwr.ss6703a1.

Trenkić, M., Popović, J., Kopitović, V., Bjelica, A., Živadinović, R., Pop-Trajković, S., 2016. Flexible GNRH antagonist protocol vs. long GNRH agonist protocol in patients with polycystic ovary syndrome treated for IVF: comparison of clinical outcome and embryo quality. Ginekol. Pol. 87 (4), 265–270.

WHO, 2014. Infecundity, Infertility, and Childlessness in Developing Countries. Demographic and Health Surveys (DHS) Comparative Reports No. 9.

WHO, 2020. Infertility. World Health Organization.

Yenkie, K.M., Diwekar, U., 2012. Stochastic optimal control of seeded batch crystallizer applying the ITO process. Ind. Eng. Chem. Res. 52 (1), 108–122. doi:10.1021/ie300491v.

Yenkie, K.M., Diwekar, U.M., Bhalerao, V., 2013. Modeling the superovulation stage in in vitro fertilization. IEEE Trans. Biomed. Eng. 60 (11), 3003–3008. doi:10.1109/TBME.2012.2227742.

Yovich, J.L., Alsbjerg, B., Conceicao, J.L., Hinchliffe, P.M., Keane, K.N., 2016. Pivet RFSH dosing algorithms for individualized controlled ovarian stimulation enables optimized pregnancy productivity rates and avoidance of ovarian hyperstimulation syndrome. Drug Des. Dev. Ther. 10, 2561. doi:10.2147/DDDT.S104104.